A Numerical Study of the behaviour on Lock Volume Variations in Lock-Exchange Density Current In Cold Fresh Water.

Abstract

The behaviour of warm discharge through lock-exchange was investigated numerically, with the assumption that density was taken as a quadratic function of temperature. Simulations were conducted eleven different times varying barrier position. This work as presented here is practical and can also enhance policy making towards the protection of the aquatic ecosystems. Such behaviours are evident in lakes, especially in holomictic lakes and warm discharge from thermoelectric power generating plants. The sudden increase in water temperature after discharge may leads to "thermal shock" killing aquatic life that has become acclimatised to living in a stable temperate environment. The aim of this investigation is to better fathom and as well, gain more insight into such flows. The results show that regimes of flow is dependent on the size of the lock volume. The general behaviours here are dependent on lock volume, density difference and Reynolds number. Effects of back reflected waves on the propagation speed was not significant for small lock volume simulations. A rapid collapsing behaviour of fluid was noticed for simulations with small lock volume, and the velocity decreases with increase in lock volume in this same phase. Propagation speed is not totally independent of the lock volume. Cabbeling was also key at the point where water masses meet, and as well the development of Kelvin-Helmholtz instabilities. Relations that describes the various regimes of flow are given in Table (1 - 11). Though, there are little variations in the scaling laws as compared to the earlier studied cases where density difference was by the means of salt water. Lastly, it will be interesting if measures can be taken to eliminate the effect of this back reflected waves in other to properly fathom the behaviour in the propagation of the frontal speed after the slumping phase.

Keywords: Density current, Cabbeling, Regimes of flow, Temperature of maximum density.

1 Introduction

Gravity current are natural behaviours that are frequently encountered in our environment and also in some man-made situations. These currents are likely to appear whenever a flow fluid with a particular density propagates into an ambient fluid with a different density, where the motion is required to be in the horizontal direction [1, 2]. Density differences in such flows are as a result of changes in temperature, salinity or concentration of suspended particles [3]. Examples of such behaviours are evident when part of the water in some river mouth, lakes, etc. come in contact. Because some of the water in these areas are saltier or colder and in turn will form density current as lighter fluid flow to the surface. In some cases, the water in such areas also contains more suspended sediment than the surrounding water. Thus, these currents are also known to be responsible for the transportation of sediments in reservoirs [2, 3] . Gravity current can also be formed when the door of a heated room is opened for ventilation. In this case, we can observed that cold air from outside flows into the room, displacing the less dense air on the floor inside. These currents can also be found in thunderstorm outflows, sea-breeze fronts, discharge of industrial waste water into rivers, lakes or oceans, volcanic clouds, etc., [1, 2, 3, 21, 22]. We can also view [4, 5, 6, 7] for more examples of such flows.

Quite a number of literature has been given in this area of research and also examined theoretically, experimentally and numerically together with some mathematical relations and values that describes the propagation speed and spreading distance of such currents. Different regimes of flow are also identified that describe the flow behaviour [2, 5, 8, 9]. Nevertheless, [10, 11, 12] have also considered density currents, using a simplified theoretical model that describes the evolution of the frontal head and a derivation of theoretical model for the initiation of a steady two-dimensional density current in a rectangular channel. And lastly, a numerical solution by using the shallow-water equation for a two-layer fluid that has to do with an empirical front condition. But then, in most of the configurations, the lock-exchange method is used (see Fig. 1): as this enables such flow scenarios over the rough and smooth horizontal surfaces and as well as the inclined surfaces [2]. In such experimental cases, salt is mostly used to create the density difference in fresh water and example of such investigation with the lock-exchange configuration include [8, 9, 13 - 18].

Furthermore, when water masses on either side of the temperature of maximum density (T_m) come in contact, cabbeling will occur even as the various fluids advance in their opposite directions. Where the most dense fluid on the floor will form a density current spreading outwards. This behaviour is also evident in lakes, especially in holomictic lakes and warm discharge from thermoelectric power generating plants. We can see [5, 19, 20] for more insights and a more detailed literature review in other to minimise repetition. But then, density currents flows through lock-exchange whereby density variation is as a result of temperature difference had not received much attention as compared to that with salt water that is widely used [2, 8].

Research has shown that gravity currents usually undergo either two or three distinct phases of flow and these include: a slumping phase, self-similar phase and viscous phase [12, 21, 22]. As also recorded in the literature of [13, 22] that after the instantaneous removal of the gate, an initial adjustment phase where the advancing head varies with approximately constant velocity. Followed immediately by the second phase after the ambient fluid had reflected at the rear wall, it in turn overtakes the penetrating head of the current. If only the lock-exchange experiment was carried out in a finite confined channel [5]. At this point in the flow, the penetrating head advances as $t^{2/3}$, but decreases with front speed as $t^{-1/3}$, where t is the time after which the gate was removed. Lastly, is the phase where viscous effects overcome inertial effects and the current front velocity decreases more rapidly as $t^{-4/5}$, with front position advancing as $t^{1/5}$ [23].

However, we have recently carried out a Numerical investigation entitled "Density Current Simulations In Cold Fresh Water And Its Cabbeling phenomenon: A Comparative Analysis With Given Experimental Results", where we have extensively discussed the behaviour of such flows, taken density as a quadratic function of temperature. Three regimes of flow were also identified together with the development of Kelvin-Helmholtz instability as recorded in earlier investigations. Relations were drawn that describes the propagation speed of the frontal head and as well as the distance traveled with respect to time [2]. Though, these Relations were drawn from simulations with computational domain length $L = 10000$, i.e., $0 \leq X \leq 10000$, with a domain height $H = 1200$ i.e., $0 \leq Y \leq 1200$ with barrier position $0.07L/14$. We have also recorded that the collapsing velocity of the denser fluid within the first time frame was high, higher than every fluid movement elsewhere. And concluded that the general behaviours as recorded are

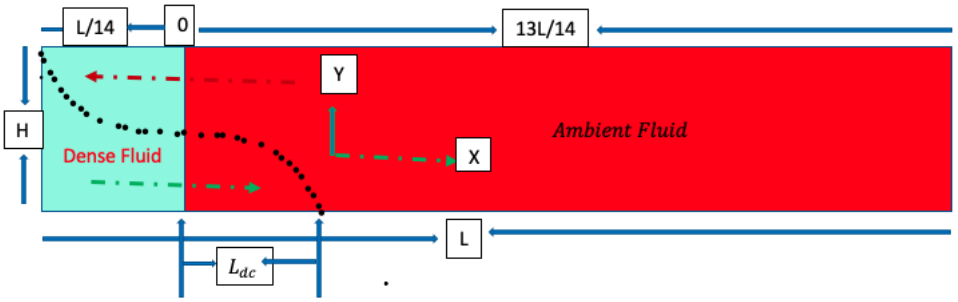

Fig. 1: Schematic presentation of Lock-exchange flow in a channel of length L and height H. The dotted line gives the interface between the two fluids some time after the release.

dependent on lock volume, density difference and Reynolds number [2], as also recorded in the literature of [8].
But then, we noticed that there are variations in the scaling laws as compared to the earlier studied cases [8, 18, 22, 23]. Though, we have claimed that the velocity of the gravity current is highly influenced by density difference and lock volume (i.e., velocity increases with increasing density difference for those where density variation is as a result of salt water and a considerably high lock volume) [2]. Thus, the consideration of barrier position is key, being that the lock volume is also believed to be a factor. Hence, we believe also that the two cases as considered in the recent study is not enough and as such, we have considered this as a limitation. Then, there is the need to carryout another investigation varying barrier position to fathom, if the speed of the current is really and also dependent on the barrier position. [24, 25] have also studied density current flows through lock-exchange, where density variation was as a result of temperature difference. But their work did not give a detailed description on the evolution of the frontal head and did not also obtain empirical scaling laws that describes the propagation speed of the current. We have considered these limitations especially, varying barrier position to be very important, and for this reason, we will carryout a detailed investigation so as to better fathom and as well, gain more insight into such studies. Thus, taken into consideration here is the motion of fluids with T_m (which is $3.98^{\circ}C$ for fresh water at atmospheric pressure, (i.e., approximately $4^{\circ}C$ in some numerical calculations)) initially at rest but separated by a vertical barrier in a rectangular domain with an ambient fluid with temperature zero. As usual, It is expected that difference in the hydrostatic pressure will result in the denser fluid flowing in one direction along the floor once the barrier is lifted up. Meanwhile the less dense fluid will flow in the opposite direction horizontally along the upper part of the domain, and this in turn create a mixing layer between the two fluids as they interact with each other [2, 5]. However, the interaction process will continue even as the most dense fluid is located at the lower part with a frontal or leading head penetrating the ambient fluid. This will continue until the dense but warm fluid will mix to a point where both fluids attain the same temperature [2, 5].
Our present investigation is based on numerical simulations that uses the lock exchange method with the assumption that density is a quadratic function of temperature. Density current which contains a dense but warm fluid in this case is expected to mix further as it spreads outward on the floor. This will continue until the dense fluid will mix to a point where it attain the same temperature with the ambient fluid [2, 5].

Computational domain length and height will be kept constant, where length $L = 10000$, i.e., $0 \leq X \leq 10000$, and a domain height $H = 1200$ i.e., $0 \leq Y \leq 1200$ but varying barrier position between $0.14L/14$ and $2.1L/14$. The input fluid (lock volume) temperature is $\phi_{in} = 1$ on the right hand side. Meanwhile, on the left hand side (ambient fluid) is $\phi_{in} = 0$. Where L is the total length of the computational domain and ϕ_{in}, the initial temperature on the various sides of the barrier.

2 Model Formulation and Governing Equations

The behaviour of the frontal head in density currents as denser fluid spread outwards on the floor after the lock release due to the nonlinear relation between density ρ and temperature T is very important. Thus, the relation below is useful for this study,

$$\rho = \rho_m - \beta(T - T_m)^2 \tag{1}$$

This, we believe gives a very good fit to the experimentally determined density of fresh water at temperature below $10^{\circ}C$ if we consider $T_m = 3.98^{\circ}C$, $\rho_m = 1.000 \times 10^3\ kg.m^{-3}$ and $\beta = 8.0 \times 10^{-3}\ kg.m^{-3}(^{\circ}C)^{-2}$ [26, 27] and all other fluid properties (e.g. viscosity, thermal diffusivity) are assumed constant. We also assume that the flow is time dependent and two dimensional, and that the liquid property is constant except for the water density, which changes with temperature and in turn results to the buoyancy force. We can non-dimensionalise the coordinates x, y, velocity components u, v, time t, pressure p and temperature T by

$$U = \frac{u}{U_*} \quad V = \frac{v}{U_*} \quad X = \frac{x}{H} \quad Y = \frac{y}{H} \quad \tau = \frac{t}{\frac{H}{U_*}} \quad P = \frac{p}{\rho U_*^2}$$

$$\phi = \frac{T - T_\infty}{T_m - T_\infty}, \tag{2}$$

where x and u are horizontal, y and v are vertical; $U_* = \sqrt{\frac{\rho_\infty - \rho)}{\rho} H}$ is the relative frontal velocity and domain height H. We also define dimensionless parameters, the Reynolds Re, Prandtl Pr and Froude Fr numbers, by

$$\nu = \frac{\mu}{\rho} \quad \alpha = \frac{k}{\rho c_p} \quad Re = \frac{U_* H}{\nu} \quad Pr = \frac{\nu}{\alpha} \quad Fr^2 = \frac{\rho_m U_*^2}{g\beta(T_m - T_\infty)^2 H}, \tag{3}$$

where ν and α are the respective diffusivities of momentum and heat, and μ is viscosity, k is thermal conductivity and c_p is specific heat capacity. In terms of these dimensionless variables and parameters, the continuity equation, the horizontal and vertical momentum equations and the thermal energy equation are given as

$$\frac{\partial U}{\partial X} + \frac{\partial V}{\partial Y} = 0 \tag{4}$$

$$\frac{\partial U}{\partial \tau} + U\frac{\partial U}{\partial X} + V\frac{\partial U}{\partial Y} = -\frac{\partial P}{\partial X} + \frac{1}{Re}\left(\frac{\partial^2 U}{\partial X^2} + \frac{\partial^2 U}{\partial Y^2}\right) \tag{5}$$

$$\frac{\partial V}{\partial \tau} + U\frac{\partial V}{\partial X} + V\frac{\partial V}{\partial Y} = -\frac{\partial P}{\partial Y} + \frac{1}{Re}\left(\frac{\partial^2 V}{\partial X^2} + \frac{\partial^2 V}{\partial Y^2}\right) + \frac{1}{Fr^2}[\phi^2 - 2\phi] \tag{6}$$

$$\frac{\partial \phi}{\partial \tau} + U\frac{\partial \phi}{\partial X} + V\frac{\partial \phi}{\partial Y} = \frac{1}{RePr}\left(\frac{\partial^2 \phi}{\partial X^2} + \frac{\partial^2 \phi}{\partial Y^2}\right) \tag{7}$$

The terms U_{dc} and L_{dc} are used to describe the propagating speed and spread length of the density current. Our initial conditions are an undisturbed, homogeneous medium as also given in [2].

$$U = 0, \quad V = 0, \quad \phi = 0, \quad for \quad \tau < 0 \tag{8}$$

For $\tau \geq 0$ we have boundary conditions as follows. On the side walls:

$$U = 0, \quad V = 0, \quad \frac{\partial \phi}{\partial X} = 0 \tag{9}$$

At the plume source:

$$U = U_*, \quad V = 0, \quad \phi_{in} = 1 \text{ for } L/14 \text{ and } 0.07L/14 \text{ and } \phi_{in} = 0 \text{ for } 13L/14 \text{ and } 13.93L/14,$$
$$\text{for} \quad X = 0, \, at \, Y = H \tag{10}$$

Table 1: Relations describing the propagation speed of the density current U_{dc} as a function of time τ_n for simulations at barrier position $0.14L/14$

Regime of Flow	U_{dc} Formula	Regression Coefficient R^2
1st	$\approx 1.3935\tau_n^{0.9138}$	≈ 0.9882
2nd	$\approx 2932.6\tau_n^{-0.936}$	≈ 0.9847
3rd	$\approx 338.74\tau_n^{-0.482}$	≈ 0.9495

On the floor of the domain:

$$U = 0, \quad V = 0, \quad \frac{\partial \phi}{\partial Y} = 0 \tag{11}$$

At the top of the domain:

$$\frac{\partial U}{\partial Y} = 0, \quad V = 0, \quad \frac{\partial \phi}{\partial Y} = 0 \tag{12}$$

The Reynolds number $Re = 50$, Froude number $Fr = 1$ and Prandtl number $Pr = 11$ will be fixed throughout this investigation. The dimensionless temperature $\phi_{in} = 1$ on the right hand side is equivalent to a discharge at $4°C$ into an ambient at $0°C$. Numerical solution of the above equations is by means of COMSOL Multiphysics software. This commercial package uses a finite element solver with discretization by the Galerkin method and stabilisation to prevent spurious oscillations. We have used the "Extremely fine" setting for the mesh. Time stepping is by COMSOL's Backward Differentiation Formulas. Further information about the numerical methods is available from the COMSOL Multiphysics website [28]. Results will be illustrated mainly by surface temperature plots of dimensionless temperature on a colour scale from dark red for the ambient temperature $\phi = 0.0$, through yellow to white for the source temperature $\phi = 1$. Note that $\phi = 1.0$ corresponds to the temperature of maximum density.

3 Results

The behaviour of warm but dense fluid, discharged at $4°C$ through lock-exchange in cold fresh water was investigated and shown in Figure 2, & 3 . Reynolds number $Re = 50$, Froude number $Fr = 1$ and Prandtl number $Pr = 11$, are kept fixed throughout the study which is similar to those by [2]. However, simulations here in this case are carried out eleven times, varying barrier position between $0.14L/14$ and $2.1L/14$; and keeping the computational domain length and height fixed. Where length $L = 10000$, i.e., $0 \leq X \leq 10000$, and a domain height $H = 1200$ i.e., $0 \leq Y \leq 1200$.
The evolution of temperature field for $\phi_{in} = 1$ within the time frame $0 \leq \tau \leq 425$ is only shown in this case, because the results here show some sort of similarities as compared with those in [2]. Except for the propagation speed that vary with lock volume which is the primary focus of this present investigation. After the release of this lock volume, a rapid collapsing behaviour of this fluid was noticed within the first few time interval for the simulations with a small lock volume. Meanwhile, the rapid movement of fluid in this same phase decreases with increase in the lock volume (see Fig. 4(a), 5(a), 6(a), 7(a), 8(a), 9(a), 10(a), 11(a), 12(a), 13(a) and 14(a)). Cabbeling process also commenced immediately after the lock release, at the point where the water masses meet even as the denser fluid on the right hand side began to form density current (see Fig. 2(b)). It is worth noting that the fluid movement in the first phase (regime) is not totally independent of the lock volume here, where density difference is as a result of temperature. This is also evident in Table 1 - 11, where we have obtained some empirically determined data set that represent the best fit power laws obtained by linear regression of $logU_{dc1}$ on $log\tau_n$.

Table 2: Relations describing the propagation speed of the density current U_{dc} as a function of time τ_n for simulations at barrier position $0.28L/14$

Regime of Flow	U_{dc} Formula	Regression Coefficient R^2
1st	$\approx 1.4214\tau_n^{0.9126}$	≈ 0.9775
2nd	$\approx 651.76\tau_n^{-0.589}$	≈ 0.9733
3rd	$\approx 181.38\tau_n^{-0.322}$	≈ 0.8964

Table 3: Relations describing the propagation speed of the density current U_{dc} as a function of time τ_n for simulations at barrier position $0.42L/14$

Regime of Flow	U_{dc} Formula	Regression Coefficient R^2
1st	$\approx 1.7268\tau_n^{0.8667}$	≈ 0.9689
2nd	$\approx 447.55\tau_n^{-0.479}$	≈ 0.9757
3rd	$\approx 292.59\tau_n^{-0.387}$	≈ 0.5504

Table 4: Relations describing the propagation speed of the density current U_{dc} as a function of time τ_n for simulations at barrier position $0.56L/14$

Regime of Flow	U_{dc} Formula	Regression Coefficient R^2
1st	$\approx 1.6978\tau_n^{0.8284}$	≈ 0.97
2nd	$\approx 159.48\tau_n^{-0.266}$	≈ 0.9776
3rd	$\approx 196.94\tau_n^{-0.308}$	≈ 0.9282

Table 5: Relations describing the propagation speed of the density current U_{dc} as a function of time τ_n for simulations at barrier position $0.7L/14$

Regime of Flow	U_{dc} Formula	Regression Coefficient R^2
1st	$\approx 1.9947\tau_n^{0.7415}$	≈ 0.9947
2nd	$\approx 135.94\tau_n^{-0.258}$	≈ 0.824
3rd	0	0

Table 6: Relations describing the propagation speed of the density current U_{dc} as a function of time τ_n for simulations at barrier position $0.84L/14$

Regime of Flow	U_{dc} Formula	Regression Coefficient R^2
1st	$\approx 2.14\tau_n^{0.699}$	≈ 0.9462
2nd	$\approx 85.221\tau_n^{-0.173}$	≈ 0.5974
3rd	0	0

Table 7: Relations describing the propagation speed of the density current U_{dc} as a function of time τ_n for simulations at barrier position $0.98L/14$

Regime of Flow	U_{dc} Formula	Regression Coefficient R^2
1st	$\approx 2.4412\tau_n^{0.6546}$	≈ 0.9514
2nd	$\approx 63.548\tau_n^{-0.109}$	≈ 0.6299
3rd	0	0

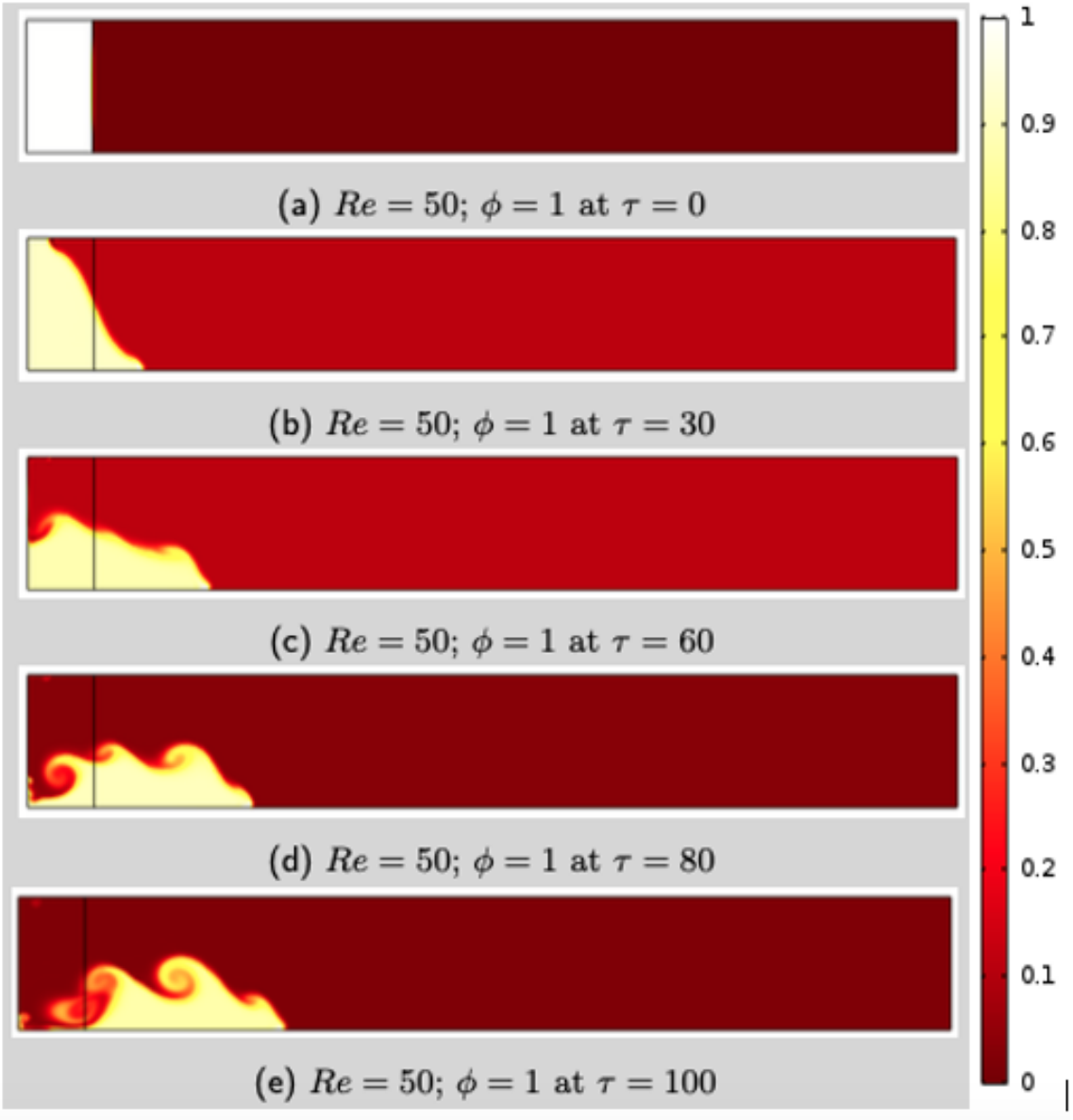

Fig. 2: Evolution of temperature field in the Density current for $Fr = 1$ and Reynolds number $Re = 50$ with $\phi = 1$ at time $0 \leq \tau \leq 100$

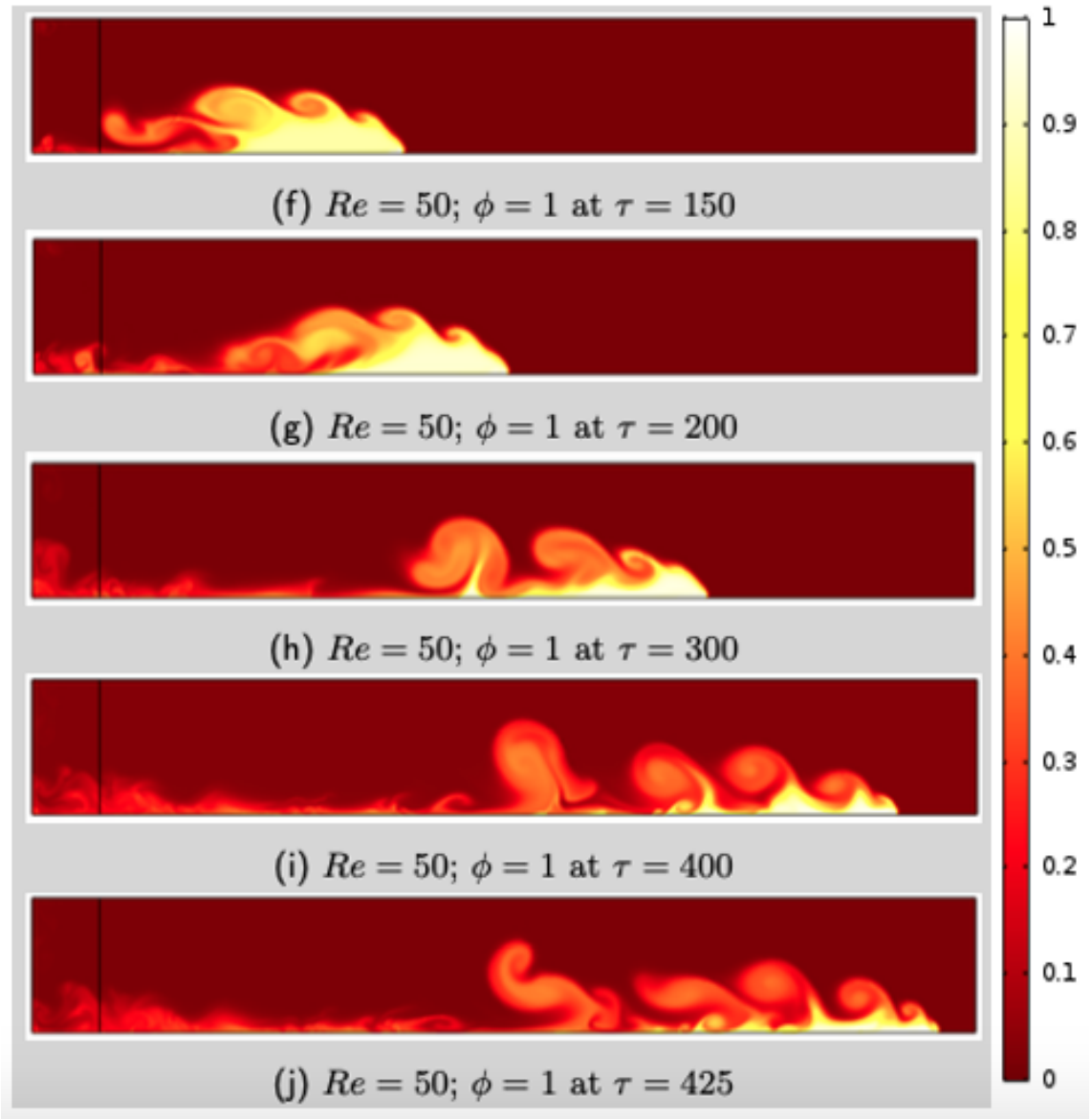

Fig. 3: Evolution of temperature field in the Density current for $Fr = 1$ and Reynolds number $Re = 50$ with $\phi = 1$ at time $150 \leq \tau \leq 425$

This we believed to be the first regime as also evident in (Fig. 4(a), 5(a), 6(a), 7(a), 8(a), 9(a), 10(a), 11(a), 12(a), 13(a) and 14(a)). The fluid movement as observed in the collapsing phase (first phase) of those currents with small lock volume seem to be higher than every fluid movement elsewhere. Afterwards, the development of Kelvin-Helmholtz instabilities at the interaction layer between the ambient and the denser fluid was observed. A fully developed stage of these unstable structures can also be seen in Fig. 3(f - j) even as the penetrating sharp head of the current advances forward, leaving fluid that have attained $\phi_{in} = 0$ at the rear. After the denser fluid had collapsed, there was a major depletion, and most of the fluid at that point had mixed up to $\phi_{in} = 0$ especially for the simulations with small lock volume. Thus, this in turn resulted in a very slow movement as the slightly warm fluid is no longer energetic to advance quickly. This behaviour was common in those simulations with small lock volume being the fact that the mixture requires just little mixing before attaining $\phi_{in} = 0$. This is also evident in Table 1 - 3, where we have also obtained some empirically determined data set that represent the best fit power laws obtained by linear regression of $logU_{dc}$ on $log\tau_n$. This we believed to be the second regime as also evident in (Fig. 4(b), 5(b), 6(b)).

However, as lock volume increases, collapsed fluid on the floor with a frontal head could still penetrate the ambient fluid quickly, even as a ground flow of warm but dense fluid from the rear continue to replenish this head. But then, we noticed that the higher the lock volume, the rapid depletion phase disappeared, and in turn leading to a two phase flow only. This is also evident in (Fig. 8 - 14), and also in Table 5 - 11, where we have also obtained some empirically determined data set that represent the best fit power laws obtained by linear regression of $logU_{dc}$ on $log\tau_n$. This we also believed to be true because the interaction layer is thin; therefore, little water is required from the dense fluid and the ambient fluid at that level of mixing, leaving much of the undiluted denser fluid below unlike those with the small lock volume (see Fig. 2(d, e) & Fig. 3(f)) [2].

The last phase of the flow show a stepwise decreasing motion in the current even as the raging columns of the Kelvin-Helmholtz instabilities dies out at the rear (see Fig. 3(h) - (j)). This is also evident in (Fig. 4(d), 5(d), 6(d) 7(d)), and also in Table (1 - 4), where we have also obtained some empirically determined data set that represent the best fit power laws obtained by linear regression of $logU_{dc}$ on $log\tau_n$. The possible explanation to this stepwise behaviour might be as a result of the regrouping process after the raging columns of the Kelvin-Helmholtz instabilities had partitioned the denser fluid. This process is expected to continue until the denser fluid will attain the same temperature with the ambient fluid and the density current will eventually halt.

The behaviours as described here show some similarities with those given in the literature by [8, 21, 22]. That gravity currents produced by means of lock-exchange over a smooth bed show two, or three, distinct phases: slumping phase, self-similar phase and viscous phase [22], which was also observed here. However, this present investigation show that number of distinct phases of flow are dependent on the lock volume (i.e., two phases of flow when the lock volume is big and three phases of flow when the lock volume is small). Previous results have shown that the transition between slumping and self-similar phases occurs when the reflected bore overtakes the frontal head of the current, and this in turn reduces the propagation speed [8, 22]. But then, we also believe that effects of back reflected waves was not significant in the propagation speed because length of the lock volume is very short for small lock volume simulations. Thus, the traveling lighter fluid at the upper part may not have gained much momentum before the back wall. Instead, the small temperature difference between the ambient fluid and the lock volume is key, as this requires a very little mixing before mixture attain $\phi_{in} = 0$. It has also been recorded that during the self-similar phase, front position decreases in time and is a function of $t^{0.78}$ approximately, which is higher than $t^{2/3}$ as described in the literature by [22]. And that the spreading in either of the self similar phases also relates to the initial lock volume [8]. The results here also show some level of similarities as lock volume increase (see Table: 3 - 11). Though, there are variation in the scaling laws as data set were determined empirically that represent the best fit power laws obtained by linear regression of $logU_{dc}$ on $log\tau_n$. And also with the fact that density variation here is as a result of temperature difference. Whereas, density variation in previous experimental studied cases uses salt water and fresh water.

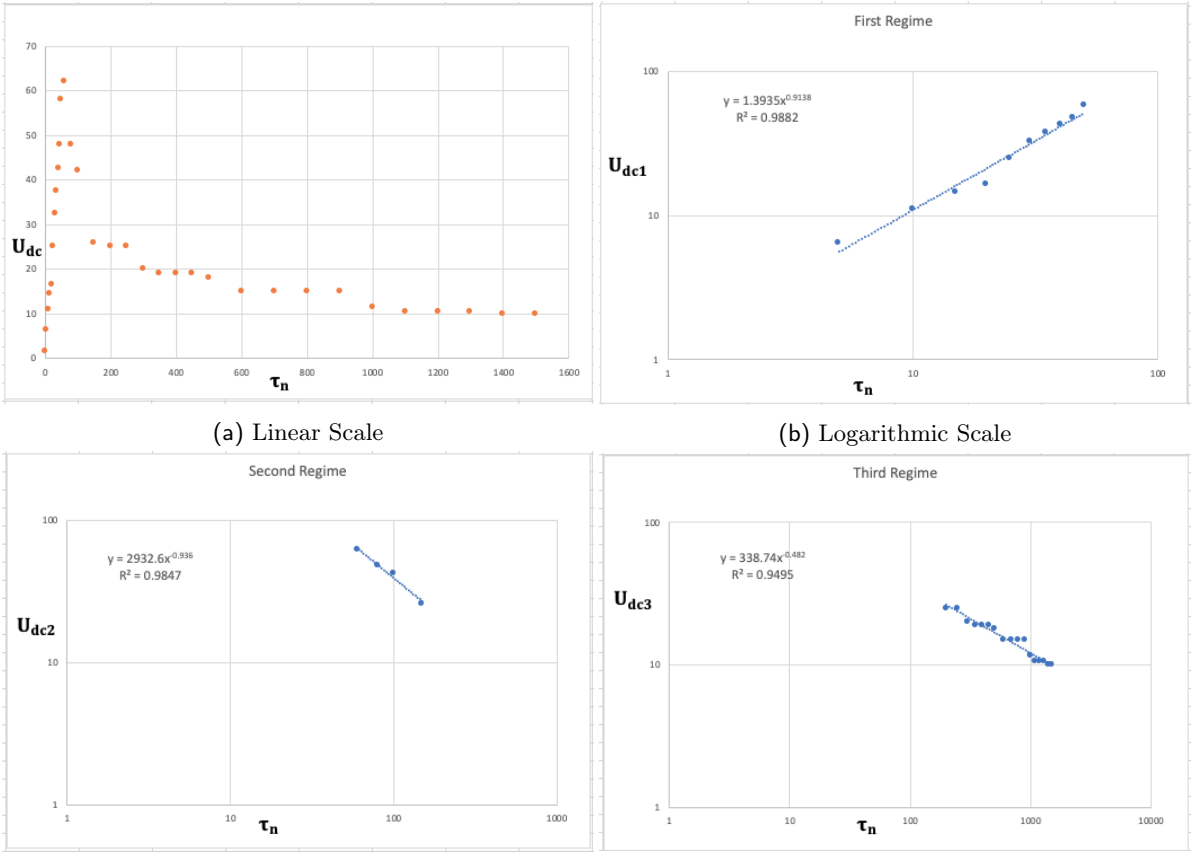

(a) Linear Scale

(b) Logarithmic Scale

(c) Logarithmic Scale

(d) Logarithmic Scale

Fig. 4: Propagation speed of the Density current U_{dc} for the different Regimes with respect to time τ_n at barrier position $0.14L/14$.

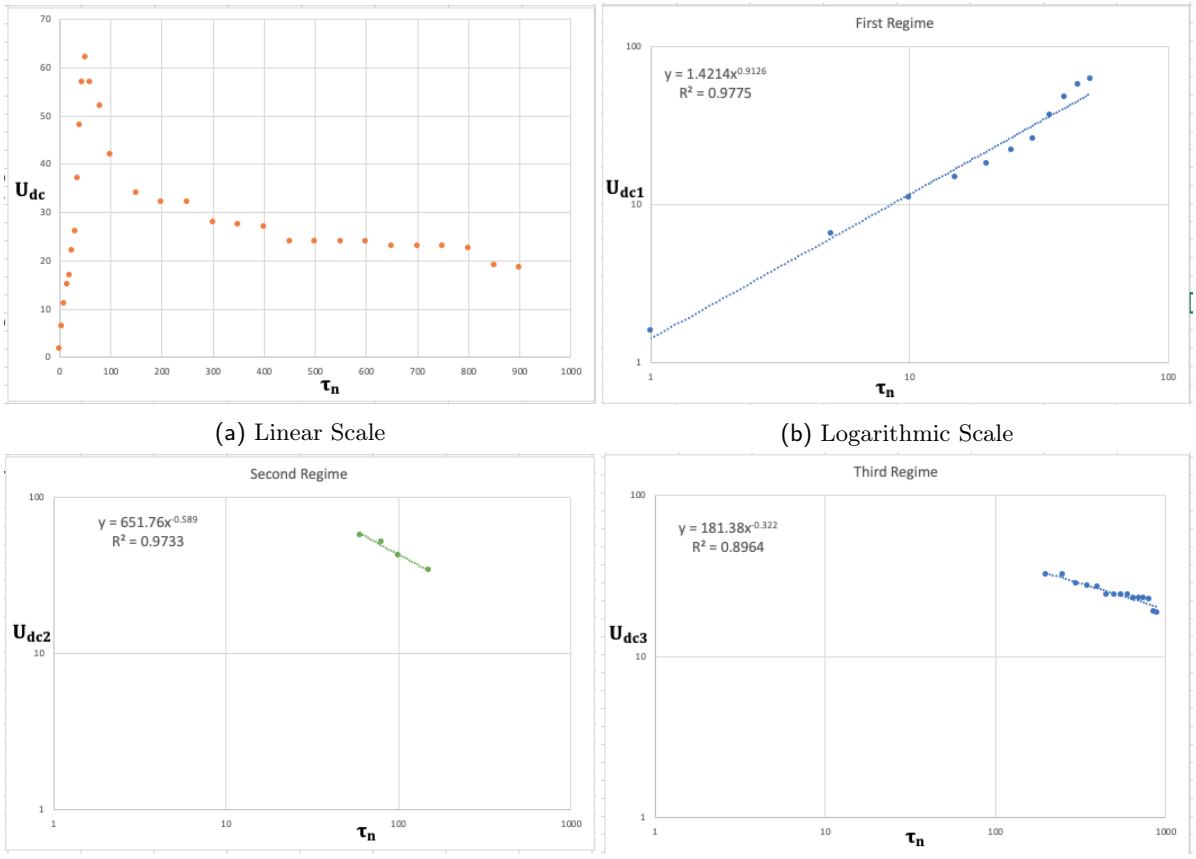

(a) Linear Scale

(b) Logarithmic Scale

(c) Logarithmic Scale

(d) Logarithmic Scale

Fig. 5: Propagation speed of the Density current U_{dc} for the different Regimes with respect to time τ_n at barrier position $0.28L/14$.

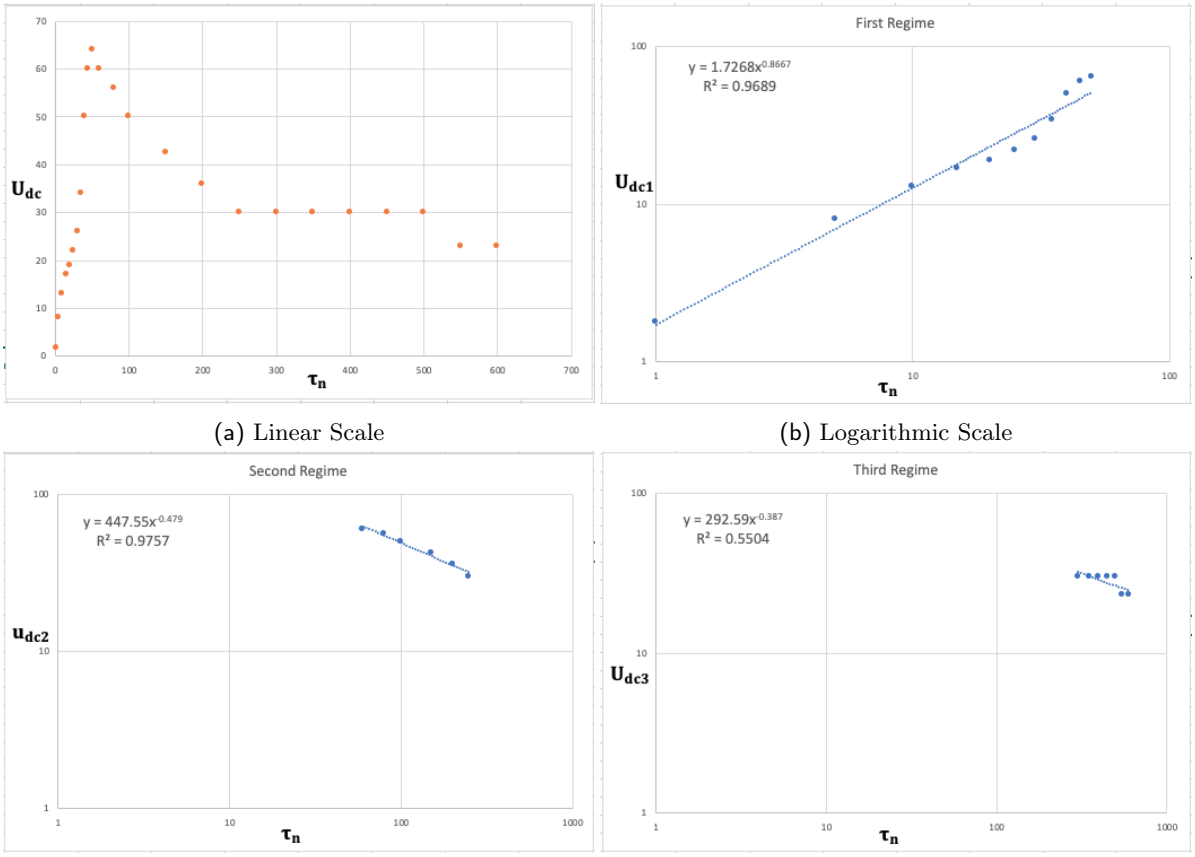

(a) Linear Scale

(b) Logarithmic Scale

(c) Logarithmic Scale

(d) Logarithmic Scale

Fig. 6: Propagation speed of the Density current U_{dc} for the different Regimes with respect to time τ_n at barrier position $0.42L/14$.

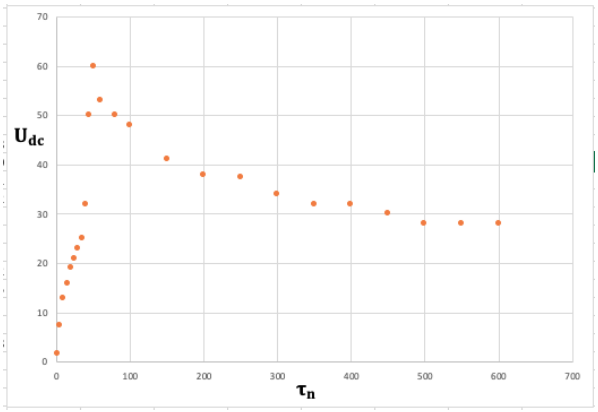

(a) Linear Scale

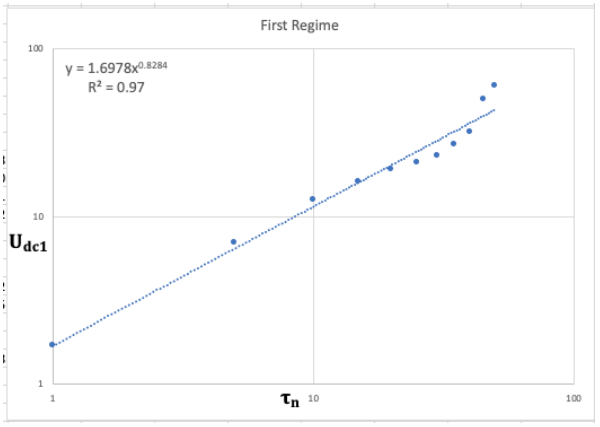

(b) Logarithmic Scale

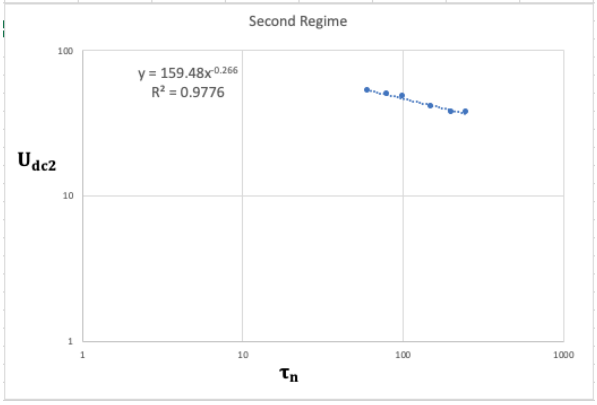

(c) Logarithmic Scale

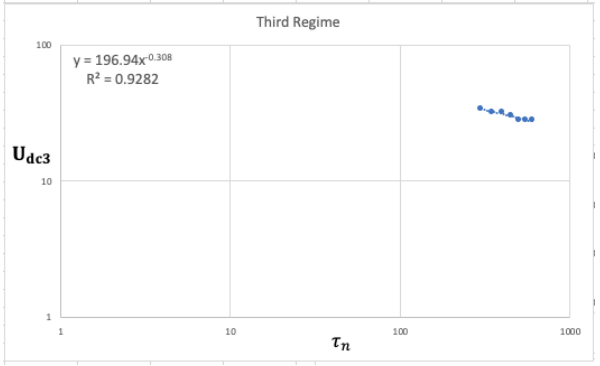

(d) Logarithmic Scale

Fig. 7: Propagation speed of the Density current U_{dc} for the different Regimes with respect to time τ_n at barrier position $0.56L/14$.

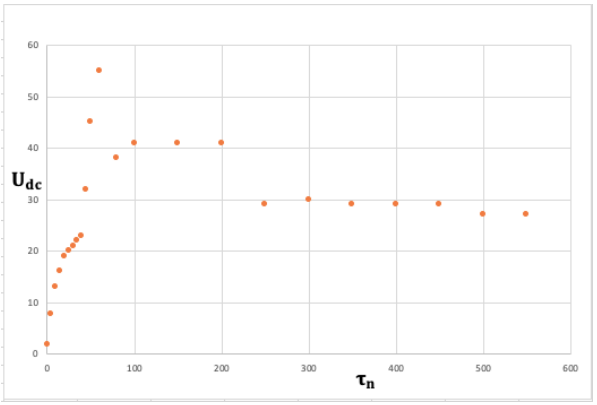

(a) Linear Scale

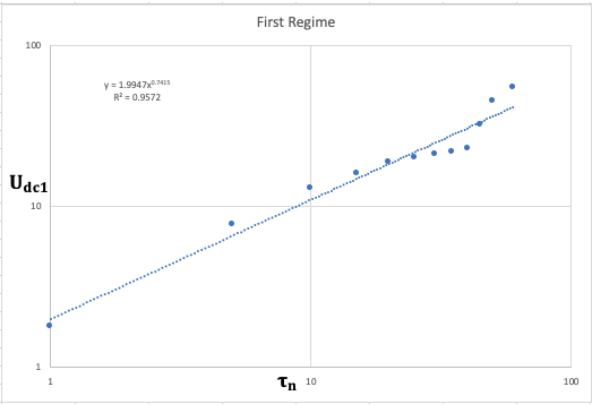

(b) Logarithmic Scale

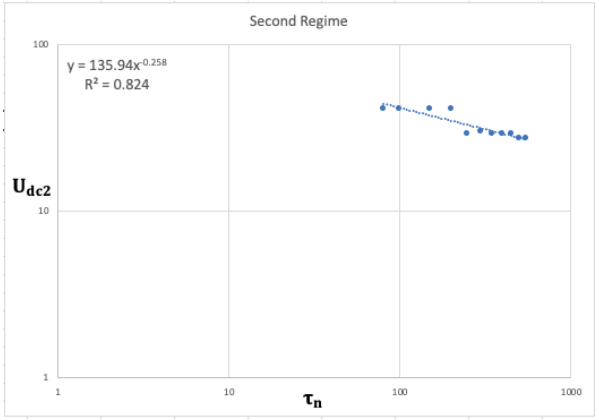

(c) Logarithmic Scale

Fig. 8: Propagation speed of the Density current U_{dc} for the different Regimes with respect to time τ_n at barrier position $0.7L/14$.

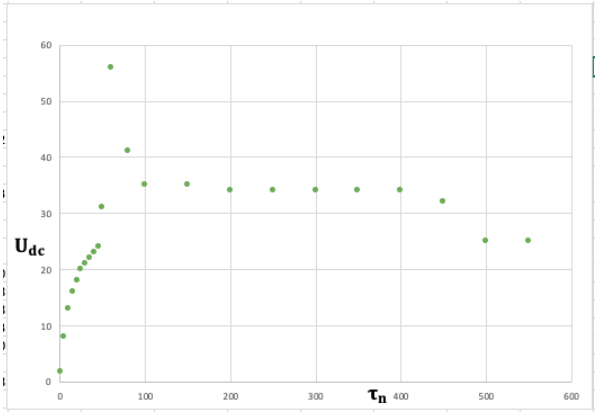

(a) Linear Scale

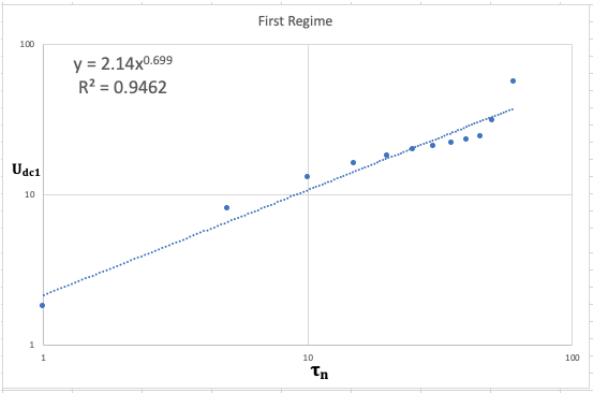

(b) Logarithmic Scale

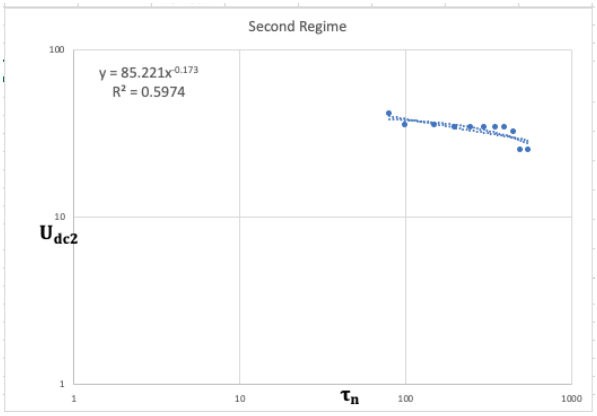

(c) Logarithmic Scale

Fig. 9: Propagation speed of the Density current U_{dc} for the different Regimes with respect to time τ_n at barrier position $0.84L/14$.

Despite the fact that mixture here requires a very little mixing before it attain the same density with the ambient fluid $\phi_{in} = 0$, the strong interaction between the two fluids also contributed to the slow movement of the current at later period. Even though the choice of numerical parameters (Reynolds number 50) for a laminar flow was suggested and ideal for the purpose of this work [2]. It is worth emphasising that in most of the lock-exchange experimental cases, salt is mostly used to create the density difference. Except for Bukreev [24, 25] who considered density variation as a result of temperature difference, but did not really give much details. Previous results have also shown that the front velocities in the slumping phase are independent of lock volume [8]. But this seem not to be the same here because as highlighted above

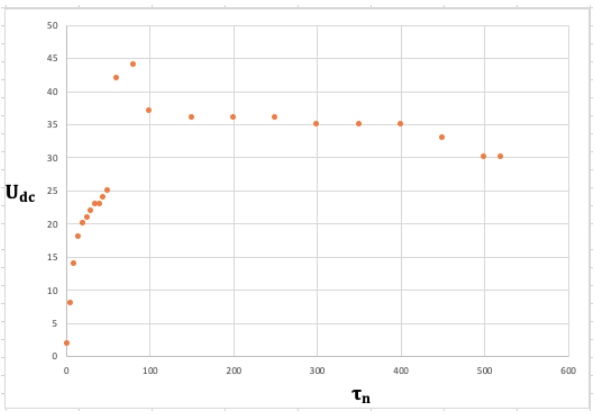

(a) Linear Scale

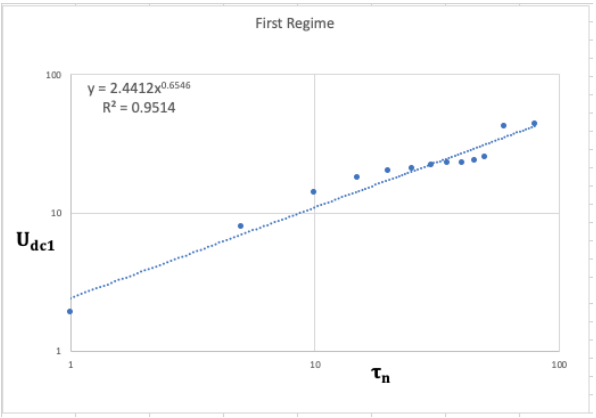

(b) Logarithmic Scale

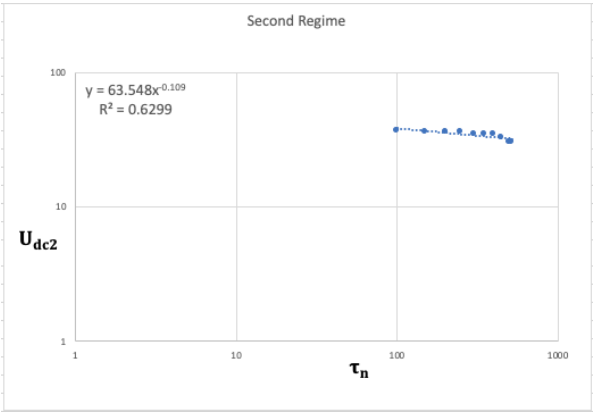

(c) Logarithmic Scale

Fig. 10: Propagation speed of the Density current U_{dc} for the different Regimes with respect to time τ_n at barrier position $0.98L/14$.

Table 8: Relations describing the propagation speed of the density current U_{dc} as a function of time τ_n for simulations at barrier position $1.12L/14$

Regime of Flow	U_{dc} Formula	Regression Coefficient R^2
1st	$\approx 2.5276\tau_n^{0.6276}$	≈ 0.9537
2nd	$\approx 65.963\tau_n^{-0.111}$	≈ 0.3883
3rd	0	0

Table 9: Relations describing the propagation speed of the density current U_{dc} as a function of time τ_n for simulations at barrier position $1.4L/14$

Regime of Flow	U_{dc} Formula	Regression Coefficient R^2
1st	$\approx 2.5308\tau_n^{0.5978}$	≈ 0.9521
2nd	$\approx 117.12\tau_n^{-0.186}$	≈ 0.4902
3rd	0	0

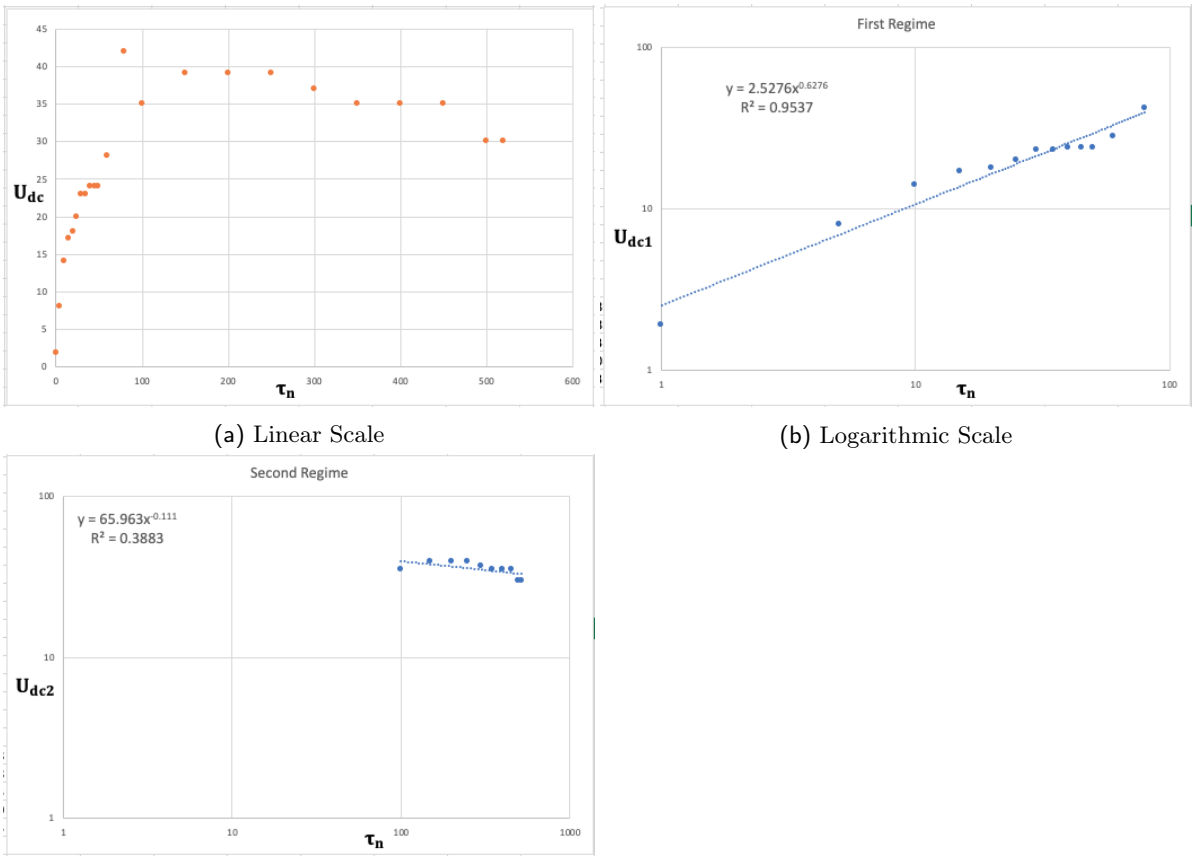

(a) Linear Scale

(b) Logarithmic Scale

(c) Logarithmic Scale

Fig. 11: Propagation speed of the Density current U_{dc} for the different Regimes with respect to time τ_n at barrier position $1.12L/14$.

Table 10: Relations describing the propagation speed of the density current U_{dc} as a function of time τ_n for simulations at barrier position $1.68L/14$

Regime of Flow	U_{dc} Formula	Regression Coefficient R^2
1st	$\approx 3.0943\tau_n^{0.5402}$	≈ 0.8921
2nd	$\approx 118.68\tau_n^{-0.197}$	≈ 0.7006
3rd	0	0

Table 11: Relations describing the propagation speed of the density current U_{dc} as a function of time τ_n for simulations at barrier position $2.1L/14$

Regime of Flow	U_{dc} Formula	Regression Coefficient R^2
1st	$\approx 3.4194\tau_n^{0.4831}$	≈ 0.8674
2nd	$\approx 259.27\tau_n^{-0.319}$	≈ 0.7497
3rd	0	0

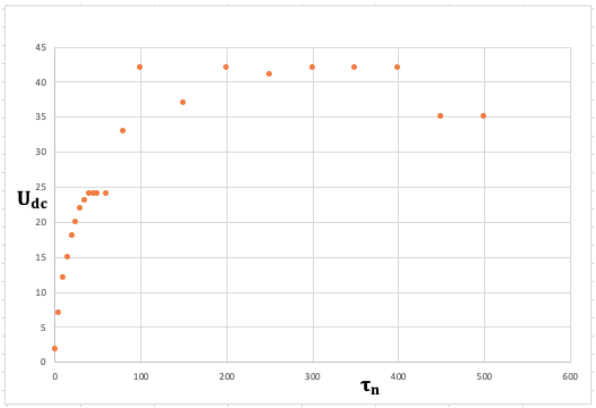

(a) Linear Scale

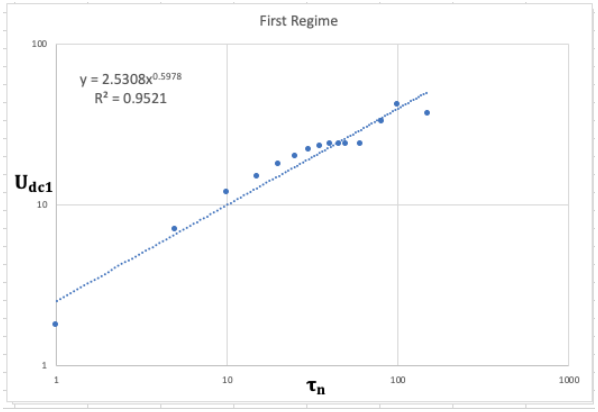

(b) Logarithmic Scale

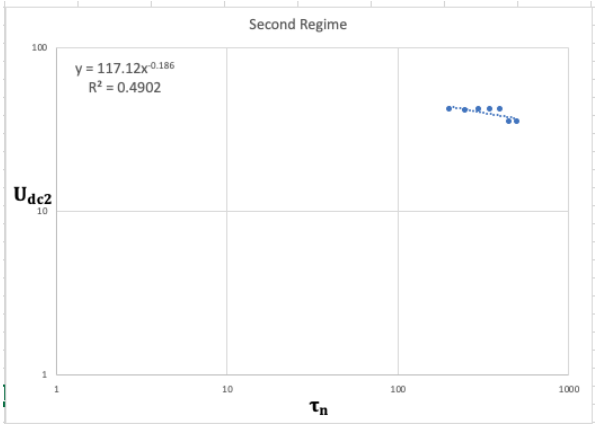

(c) Logarithmic Scale

Fig. 12: Propagation speed of the Density current U_{dc} for the different Regimes with respect to time τ_n at barrier position $1.4L/14$.

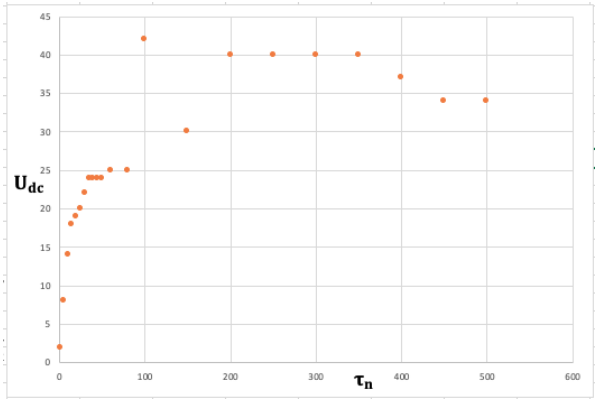

(a) Linear Scale

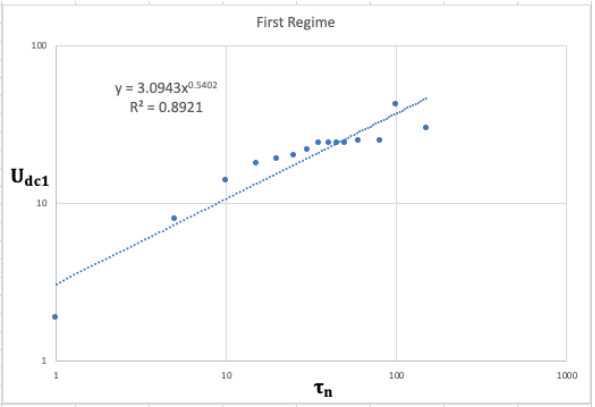

(b) Logarithmic Scale

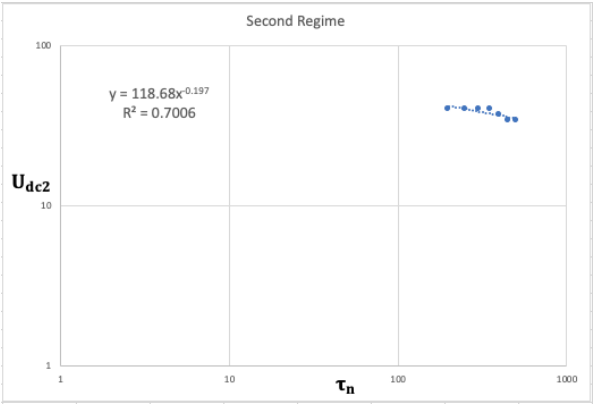

(c) Logarithmic Scale

Fig. 13: Propagation speed of the Density current U_{dc} for the different Regimes with respect to time τ_n at barrier position $1.68L/14$.

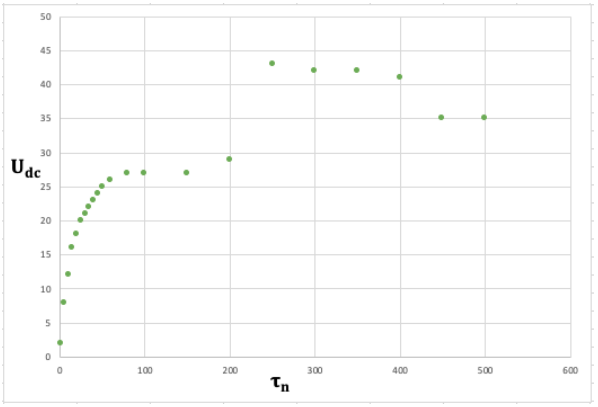

(a) Linear Scale

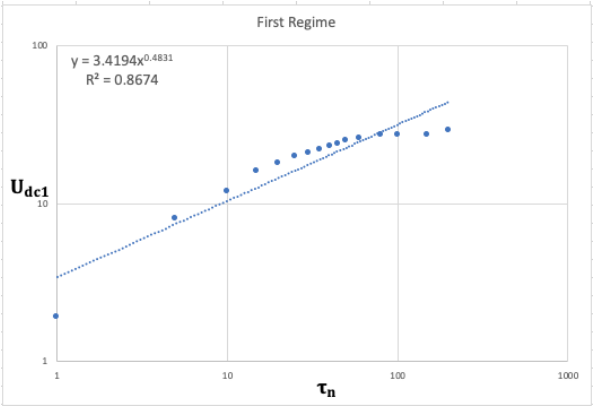

(b) Logarithmic Scale

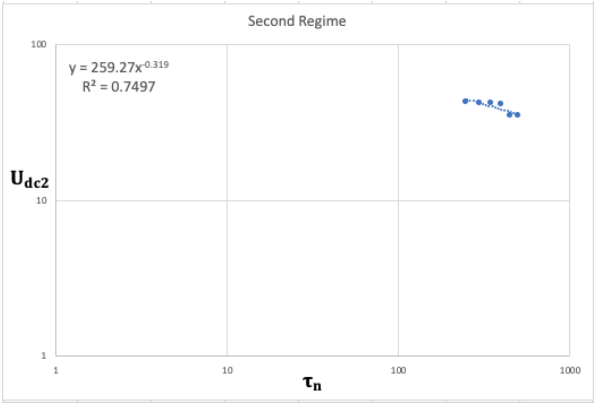

(c) Logarithmic Scale

Fig. 14: Propagation speed of the Density current U_{dc} for the different Regimes with respect to time τ_n at barrier position $2.1L/14$.

that after the lock release, a rapid collapsing behaviour of this fluid was occur for the simulations with small lock volume. Whereas, this rapid movement of fluid in this same phase decreases with increase in the lock volume (see Fig. 4(a), 5(a), 6(a), 7(a), 8(a), 9(a), 10(a), 11(a), 12(a), 13(a), 14(a) and Table (1 - 11)). Thus, the fluid movement in the first phase (regime) is not totally independent of the lock volume here, where density difference is as a result of temperature. Lastly, we have noticed that most of the scaling laws relating to gravity currents are given in terms of power laws as also presented here. But then, it may also be possible that power law does not fit well in all the flow processes [8], this we did not show for clarity. Thus, we can see this as a limitation. Furthermore, numerical simulations are mainly conducted in a finite domain and as such, most of the lock volumes are also small leading to the effect of back reflected waves on the current which is also a limitation. Thus, it will also be interesting if measures can be taken to minimise or eliminate these back reflected waves in other to properly fathom the behaviour in the propagation of the frontal speed after the slumping phase.

4 Discussion and Conclusion

The behaviour of warm discharge through lock-exchange was investigated numerically, with the assumption that density was taken as a quadratic function of temperature. Simulations were conducted eleven different times varying barrier position between $0.14L/14$ and $2.1L/14$. The results here show both two and three regimes of flow, which depends on the size of the lock volume. Though, the general behaviours here are dependent on lock volume, density difference and Reynolds number as also described by [2, 8]. A rapid collapsing behaviour of fluid was noticed in the first phase for simulations with small lock volume, and the velocity decreases with increase in lock volume in this same phase. Propagation speed here is not totally independent of the lock volume. Cabbeling was also key at the point where water masses meet with the development of Kelvin-Helmholtz instabilities. A stepwise decreasing motion was noticed, which was as a result of the development of these instabilities that later dies out at the rear as also recorded in [2]. Effects of back reflected waves was not significant in the propagation speed because length of the lock volume is very short for small lock volume simulations. Thus, lighter fluid may not have gained much momentum before the back wall. Instead, the small temperature difference between the ambient fluid and the lock volume was key, as this requires a very little mixing before mixture attain $\phi_{in} = 0$. Relations that describes the various regimes of flow are given in Table (1 - 11), which are similar to results by [2, 22]: though, there are variation in the scaling laws. But then, for those where density difference is as a result of temperature, we believe that these results are a good starting point to better fathom and as well, gain more insight into such studies. Lastly, we have noticed that most of the scaling laws relating to gravity currents are given in terms of power laws as also presented here. But then, it may also be possible that power law does not fit well in all the flow phases [8], this we did not show for clarity. Thus, we can see this as a limitation. Furthermore, numerical simulations are mainly conducted in a finite domain and as such, most of the lock volumes are also small, as this in turn perturb the free flow of the current by the back reflected waves which is also a limitation. Thus, it will also be interesting if measures can be taken to minimise or eliminate the effect of this back reflected waves in other to properly fathom the behaviour in the propagation of the frontal speed after the slumping phase. This work as presented here is practical and relevant to many fields of study and also enhances policy making towards the protection of the aquatic ecosystems. Because such discharge or introduction of warm but dense water may definitely give rise to environmental problems; where the sudden increase in the water temperature after discharge/introduction will lead to "thermal shock" killing aquatic life that has become acclimatised to living in a stable temperate environment. Researchers can also gain more knowledge in terms of the dynamics of such flows.

References

[1] Ungarish, M. (2021) *Gravity Currents and Intrusions: Analysis and Prediction.* USA, World Scientific Publishing Co. Pte. Ltd.

[2] George, M. A. and Osaisai, F. E. (2022). Density Current Simulations In Cold Fresh Water And Its Cabbeling phenomenon: A Comparative Analysis With Given Experimental Results *Current Journal of Applied Science and Technology* **41** *29* Pp. 37 - 52.

[3] Nasrollahpour, R., Jamal, H. M., Ismail, Z., Ibrahim, Z., Jumain, M., Haniffah, R. M. M and Ishak, S. M. D. (2021). *Velocity Structure of Density Currents Propagating Over Rough Beds. Water,* **13** 1460.

[4] Simpson, J. E. (1997) *Gravity Currents: In the Environment and the Laboratory.* UK, Cambridge University Press, 258 pp.

[5] George, M. A. and Kay, A. (2022). Numerical Simulations of the Cabbeling Phenomenon in Surface Gravity Currents in Cold Fresh Water *Journal of Scientific Research & Reports* **28** *1* Pp. 68 - 85.

[6] Nogueira, H. I., Adduce, C., Alves, E. and France, J. M. (2014). *Dynamics of the head of gravity currents. Journals of Environmental Fluid Mechanics,* **14** Pp. 519 - 540.

[7] Tien, N. N., Uu, D. V., Cuong, D. H., Mau, L. D., Tung, N. X. and Hung, P. D. (2020). *Mechanism of Formation and Estuarine Turbidity Maxima in the Hau River Mouth. Water,* **12** 2547.

[8] Yin, X., He, Y., Lu, C., Gao, S. and Liu, Q. (2020). *Experimental Study on Front Spreading of Lock-Exchange Gravity Current with Long Lock Length. Journal of Engineering Mechanics,* **146** *1* 04019113 (1-11).

[9] Dai, A. and Huang, Y. L. (2020). *Experiments on gravity currents propagating on unbounded uniform slopes. Environ. Fluid Mech.,* **20** *6* Pp. 1637 - 1662.

[10] Prandtl, L. (1952) *Essentials of fluid dynamics.* UK, Blackie & Son

[11] Benjamin, T. B. (1986). *Gravity currents and related phenomena. Journal of Fluid Mechanics,* **31,** *2* Pp. 209 - 248.

[12] Rottman, J. W., and Simpson, J. E. (1983). *Gravity currents produced by instantaneous releases of a heavy fluid in a rectangular channel. Journal of Fluid Mechanics,* **135,** Pp. 95 - 110.

[13] Maggi, R. M., Adduce, C. and Negretti, E. M. (2022). *Lock release gravity currents propagating over roughness elements. Environmental Fluid Mechanics,* Pp. 1 - 20.

[14] Pelmard , J., Norris, S. and Friedrich, H. (2020). *Statistical characterisation of turbulence for an unsteady gravity current. Journal of Fluid Mech.,* **901** A7.

[15] Negretti, M., Flor, J. and Hopfinger, E. (2017) . *Development of gravity currents on rapidly changing slopes. Journal of Fluid Mech.,* **833,** Pp. 70 - 97.

[16] Martin, A., Negretti, M. E. and Hopfinger, E. J. (2019). *Development of gravity currents on slopes under different interfacial instability conditions. Journal of Fluid Mech.,* **880,** Pp. 180 - 208.

[17] Dai, A. and Huang, Y. L. (2021). *Boussinesq and nonboussinesq gravity currents propagating on unbounded uniform slopes in the deceleration phase. Journal of Fluid Mech.,* **917** A23.

[18] Vardakostas, S., Kementsetsidis, S. and Keramaris, E. (2020). *Saline Gravity Currents with Large Density Difference with Fresh Water in a Valley of Trapezoidal Shape. Environ. Sci. Proc.,* **2** *(64)* Pp. 1 - 9.

[19] George, M. A. and Kay, A. (2017). Numerical simulation of a line plume impinging on a ceiling in cold fresh water *International Journal of Heat and Mass Transfer* **108** Pp. 1364 - 1373.

[20] George, M. A. and Kay, A. (2016). Warm discharges in cold fresh water: 2. Numerical simulation of laminar line plumes *Environ. Fluid Mech.* doi: http://dx.doi.org/10.1007/s10652-016-9468-x.

[21] Huppert, H. E. and Simpson, J. E (1980). *The Slumping of Gravity Currents. Journal of Fluid Mechanics* **99** Pp. 785 - 799.

[22] Nogueira, I. S. H., Adduce, C., Alves, E. and France, J. M. (2013). *Analysis of Lock-exchange gravity currents over smooth and rough beds. Journal of Hydraulic Research,* **51** *4* Pp. 417 - 531.

[23] Simpson, J. E. (1982). *Gravity currents in the laboratory, atmosphere, and ocean. JAnnu Rev Fluid Mech,* **14** *1* Pp. 213 - 234.

[24] Bukreev, I. V. (2006). *Effect of the Nonmonotonic Temperature Dependence of Water Density on the Decay of an initial Discontinuity. Journal of Applied Mechanics and Technical Physics,* **47** *1* Pp. 54 - 60.

[25] Bukreev, I. V. (2006). *Effect of the Nonmonotonic Temperature Dependence of Water Density on the Propagation of a Vertical Plante Jet. Journal of Applied Mechanics and Technical Physics,* **47** *2* Pp. 169 - 174.

[26] Moore, D. R. and Weiss, N. O. (1973). Nonlinear penetrative convection. *Journal of Fluid Mechanics,* **61** Pp. 553 - 581.

[27] Oosthuizen, P. H. and Paul, J. T. (1996). A Numerical study of the Steady State Freezing of Water in an open Rectangular Cavity. *International Journal of Numerical Methods for Heat and Fluid Flow,* **6** *(5)*, Pp. 3-16

[28] COMSOL Multiphysics Cyclopedia. *The Finite Element Method (FEM). [ONLINE] Available at: https://www.comsol.com/multiphysics/finite-element-method [Accessed 28 April 2016].*